



Electroweak phase transition in the 2HDM: collider and gravitational wave complementarity

Ajay Kaladharan

With Dr Dorival Gonçalves and Dr Yongcheng Wu

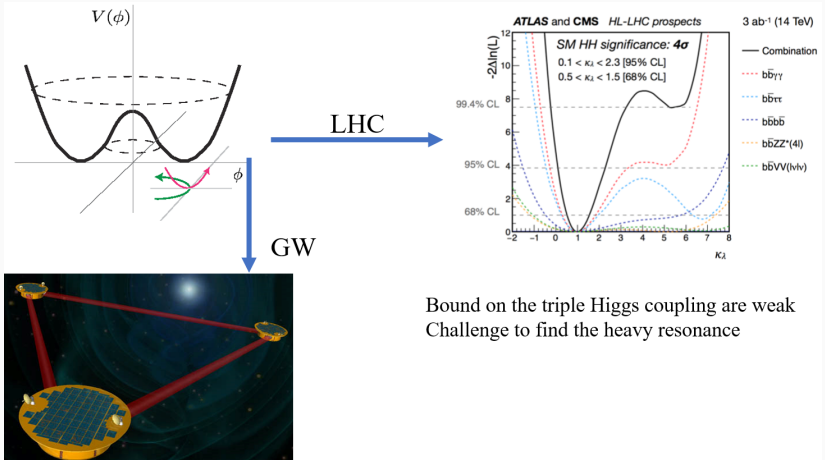
Arxiv:2108.05356

August 27, 2021

SUSY 2021

Oklahoma State University

Collider and GW Complementarity

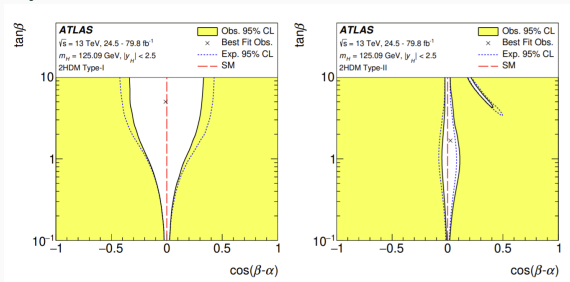


CP-conserving THDM

- CP-conserving 2HDM with a softly broken \mathbb{Z}_2 symmetry.

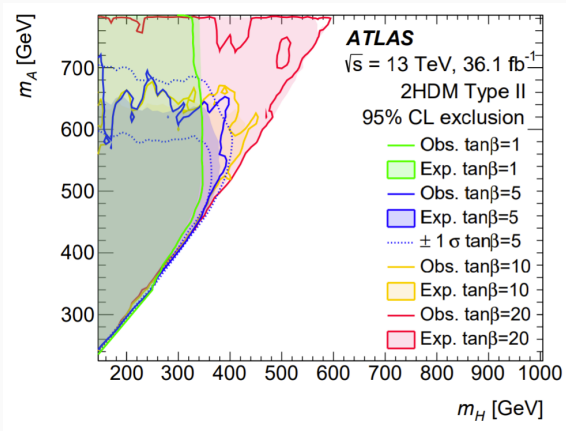
$$V(\Phi_1, \Phi_2) = m_{11}^2 \Phi_1^\dagger \Phi_1 + m_{22}^2 \Phi_2^\dagger \Phi_2 - m_{12}^2 (\Phi_1^\dagger \Phi_2 + h.c.) + \frac{\lambda_1}{2} (\Phi_1^\dagger \Phi_1)^2 + \frac{\lambda_2}{2} (\Phi_2^\dagger \Phi_2)^2 + \lambda_3 (\Phi_1^\dagger \Phi_1) (\Phi_2^\dagger \Phi_2) + \lambda_4 (\Phi_1^\dagger \Phi_2) (\Phi_2^\dagger \Phi_1) + \frac{\lambda_5}{2} \left((\Phi_1^\dagger \Phi_2)^2 + h.c. \right),$$

- \mathbb{Z}_2 symmetry transformations $\Phi_1 \rightarrow \Phi_1$ and $\Phi_2 \rightarrow -\Phi_2$



t_β - $C_{\beta-\alpha}$ plot, left side corresponds to type I and right side corresponds to type II

$$\tan\beta = \frac{v_2}{v_1}$$



$m_A - m_H$ for type II

$A \rightarrow ZH \rightarrow \ell\ell b\bar{b}$

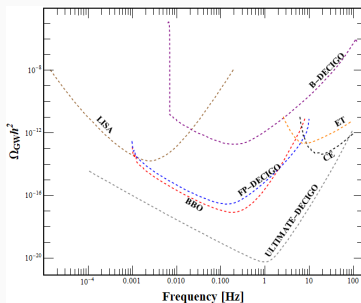
Electroweak phase transition

- To study the thermal evolution of the universe.
- Electroweak baryogenesis provides a mechanism to explain the baryon asymmetry in the universe. Baryon asymmetry can be generated at the bubble walls during first-order phase transition. The condition for strong first-order transition is given by,

(M. Shaposhnikov, 1992)

$$\xi_c \equiv \frac{v_c}{T_c} \geq 1.$$

- First-order phase transition in the early show detectable GW signals today.

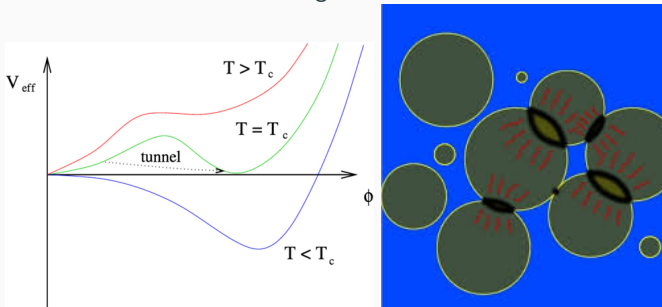


$$\begin{aligned}V_{\text{eff}}(\omega_1, \omega_2, T) &= V_0(\omega_1, \omega_2) + V_{CW}(\omega_1, \omega_2) + V_{CT}(\omega_1, \omega_2, T) + V_T(\omega_1, \omega_2) \\ &= V_0(\omega_1, \omega_2) + V_1(\omega_1, \omega_2) + V_T(\omega_1, \omega_2).\end{aligned}$$

(Philipp Basler, Margarete Muhlleitner, Jonas Muller, 2019)

First order phase transition

At the critical temperature, T_C symmetry broken and unbroken vacuum are degenerate.



$$\frac{S_3(T_n)}{T_n} \approx 140.$$

(R. Apreda, M. Maggiore, A. Nicolis, and A. Riotto, 2002)

$$\alpha = \frac{\rho_{vac}}{\rho_{rad}} = \frac{1}{\rho_{rad}} \left[T \frac{d\Delta V}{dT} - \Delta V \right]_{T_n}, \quad \beta = \left(HT \frac{d(s_3/T)}{dT} \right)_{T_n}.$$

- During the first-order phase transition, GW waves are produced from three sources bubble wall collision, sound waves and magnetohydrodynamics (MHD) solutions.

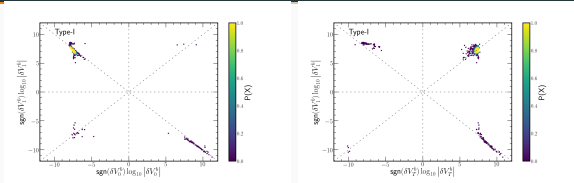
(P. Binetruy, A. Bohe, C. Caprini, and J.F. Dufaux, 2012)

$$\Omega_{GW} h^2 = \Omega_{sw} h^2 + \Omega_{turb} h^2 + \Omega_{coll} h^2.$$

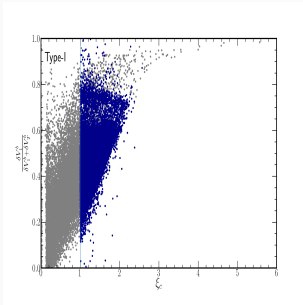
- GW signal is detectable in detector if $SNR > 10$.

$$SNR = \sqrt{\tau \int_{f_{min}}^{f_{max}} df \left[\frac{\Omega_{GW}(f) h^2}{\Omega_{sens}(f) h^2} \right]^2}.$$

Shape of the potential

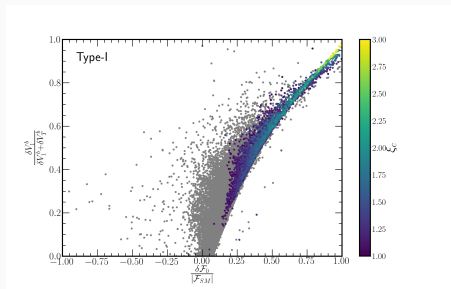


In the SFEWPT regime, $\xi_c > 1$ the phase transition is mostly one-loop driven, i.e., the effective potential barrier is dominantly generated by the one-loop term.



If the fraction of the barrier height provided by the one-loop contribution is close to 100%, the tunnelling from the false vacuum to the true vacuum is more challenging. For this reason, the universe with $\xi_c > 2.5$ trapped in the false vacuum.

Shape of the potential

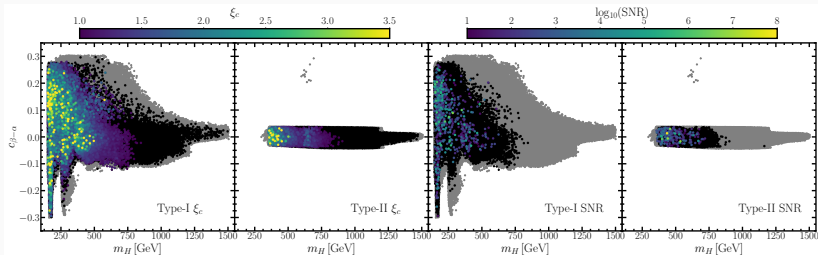


The barrier height provided by the one-loop contribution is correlated to $\Delta\mathcal{F}_0/|\mathcal{F}_0^{\text{SM}}|$ which measures the vacuum upliftment at zero temperature.

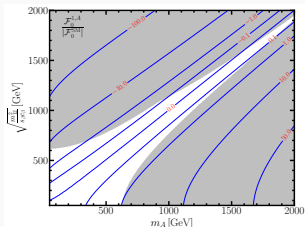
\mathcal{F}_0 is the vacuum energy density of the 2HDM at $T = 0$ defined as

$$\mathcal{F}_0 \equiv V_{\text{eff}}(v_1, v_2, T = 0) - V_{\text{eff}}(0, 0, T = 0),$$

and $\mathcal{F}_0^{\text{SM}} = -1.25 \times 10^8 \text{ GeV}^4$.

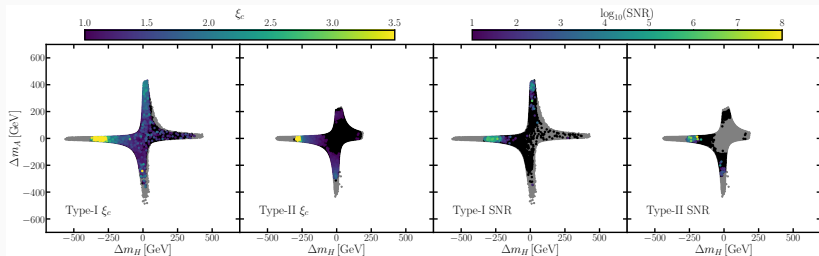


Grey: all points passing HiggsBounds and HiggsSignal. Black: all points with first order phase transition. The heat map tracks ξ_c (left) and SNR (right).



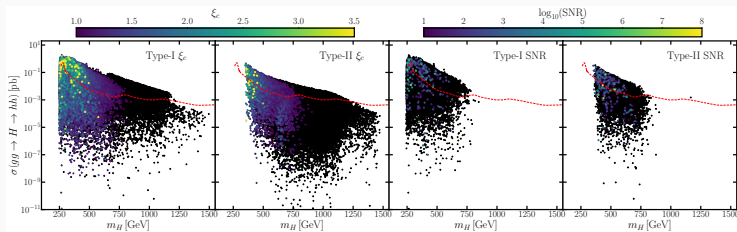
The individual contribution $\mathcal{F}_0^{1,A}/|\mathcal{F}_0^{\text{SM}}|$ from A (blue solid line) in $m_A - \sqrt{\frac{m_{12}^2}{s_{\beta} c_{\beta}}}$ plane. We assume the alignment limit. The grey shaded region is excluded by unitarity and perturbativity constraints assuming $t_{\beta} = 1$, $c_{\beta-\alpha} = 0$, and $m_A = m_{H\pm} = m_H + 100$ GeV.

$$\Delta m_H - \Delta m_A$$

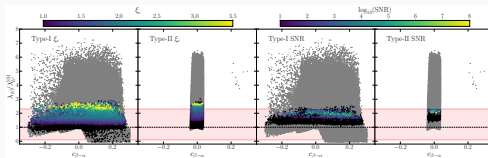


- $\Delta m_H = m_H - m_{H^\pm}$ and $\Delta m_A = m_A - m_{H^\pm}$.
- For type II, $m_{H^\pm} < 580$ GeV has been excluded by the measurements of $\text{BR}(B \rightarrow X_s \gamma)$.

Resonant and Non-Resonant di-Higgs Searches

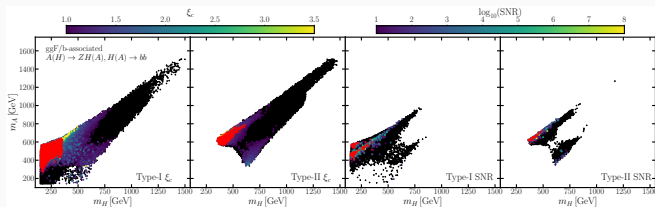


The cross section $\sigma(gg \rightarrow H) \times \text{BR}(H \rightarrow hh)$ vs. m_H . The red dashed line indicates the projected limits from ATLAS with 3000 fb^{-1} by scaling current limits.



The triple Higgs coupling normalized to SM value as function of $c_{\beta-\alpha}$. The HL-LHC projected 95% CL sensitivity for non-resonant di-Higgs production is also shown $0.1 < \lambda_{h^3}/\lambda_{h^3}^{\text{SM}} < 2.3$ (light red)

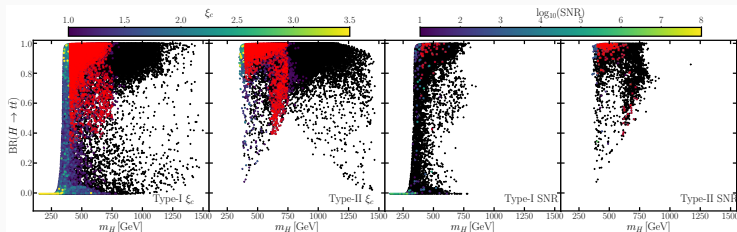
$A \rightarrow ZH$ and $H \rightarrow ZA$ Searches



The $A \rightarrow ZH$ constraints on m_H - m_A plane. The red crosses are the points that can be probed by the HL-LHC through $A \rightarrow ZH \rightarrow \ell\ell b\bar{b}$ searches, where A is produced through gluon fusion or via b -associated production

- The widely discussed $A(H) \rightarrow ZH(A)$ channel in the context of EWPT in 2HDM is still relevant but for a smaller fraction of points compared to other searches.
- Whereas the $H \rightarrow b\bar{b}$ channel generally provides the strongest limits for this channel, it quickly becomes subdominant once the scalar mass is beyond top-pair threshold.
- The $H \rightarrow WW$ channel shows smaller sensitivity as it is suppressed by $C_{\beta-\alpha}$.

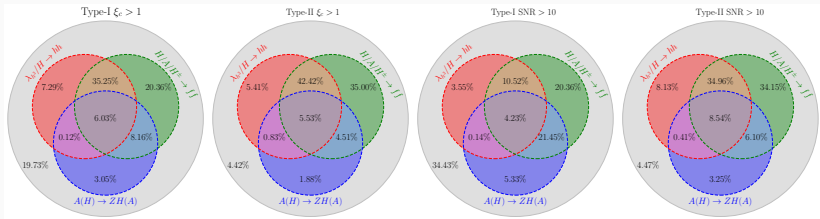
Scalar Decays to Heavy Fermions



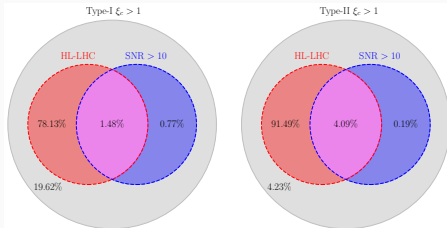
Branching fraction $BR(H \rightarrow t\bar{t})$ as function of m_H . The red crosses are the points with $\xi_c > 1$ (left panels) and $\text{SNR} > 10$ (right panels) that can be probed by HL-LHC through resonant searches decaying to top quark pair.

- The resonant searches with heavy fermionic final states is crucial for SFOPEWPT sensitivity at the HL-LHC.
- Type-II 2HDM is more constrained at the HL-LHC for $\xi_c > 1$ points as the type-II have a stronger lower bound on scalar masses favoring the $H/A \rightarrow t\bar{t}$ search.

Combined Results



The summary of the capabilities of corresponding search channels at the HL-LHC.



The summary of the capabilities of the HL-LHC and GW experiments.

- Type I and Type II have similar phase transition behaviour and GW signals.
- The barrier formation in the Higgs potential of the 2HDM is driven by the one-loop and thermal corrections, with the dominance of the one-loop terms for large order parameter $\xi_c > 1$
- Scalar decays to heavy fermions $H^\pm, H, A \rightarrow tb, tt$ is the most promising smoking gun signature for SFOEWPT at the HL-LHC, followed by the di-Higgs searches.
- In contrast to the HL-LHC, LISA is going to be sensitive to a significantly smaller parameter space region, whereas it renders to complementary sensitivities where the correspondent LHC cross-section is suppressed.

Thank you!